(3 × 20 mL). Filtrate and washings were combined and concentrated to ca. 20 mL and then applied to a silica gel column (3 cm o.d. × 33 cm). The elution of Fe_2·gable Cl_2 with CH_2Cl–MeOH (15:1) was followed by TLC (silica gel, R_f = 0.3 [CH_2Cl_2–MeOH = 15:1); UV λ_{max} (benzene) 689, 622, 572, 507, 420 nm): All fractions containing Fe_2·gable Cl_2 were combined and concentrated to 30 mL. Hexane (30 mL) was added and the mixture was slowly condensed to 20 mL and kept standing overnight in a refrigerator. Fine dark-purple crystals formed were filtered, washed with hexane (3 × 3 mL), and dried in vacuo to yield 96 mg (0.072 mmol, 82.1%) of **8d**. Fe_2·gable Cl_2 was further purified by recrystallization from toluene. (**8d**): mp >300 °C dec; ν_{max} (KBr) 2950, 2800, 1600, 1480, 1440, 1340, 1260, 1080, 1000, 900, 800, 760, 720, 700, 440, 360 cm^{-1}; FD-MS, *m/e* (rel intensity) 1331 (53, $M^+ + 3$), 1330 (91, $M^+ + 2$), 1329 (100, $M^+ + 1$), 1328 (23, M^+), 1327 (56, $M^+ - 1$), 1294 (72, $M^+ - Cl + 1$), 1259 (13, $M^+ - 2Cl + 1$); λ_{max} (benzene) 689, 622, 572, 507, 420 nm.

Fe^{II}_2·Gable (8e). All manipulations were performed in the drybox (filled with oxygen-free argon) to avoid any oxidation of Fe^{II}·porphyrin. A mixture of 2.0 mg (1.6 × 10^{-6} mol) of Fe^{III}_2·gable Cl_2 (**8d**) in 5 mL of benzene and 0.5 mL of aqueous buffer solution (0.1 M phosphate, pH 6.86) was deoxygenated by 3 freeze–pump–thaw cycles (2 × 10^{-6} torr). To the mixture 20 mg (1.1 × 10^{-4} mol) of solid $Na_2S_2O_4$ was added and the mixture was stirred vigorously for 30 min. The resulting orange-red solution of crude bisferrous gable porphyrin (**8e**) was dried over anhydrous Na_2SO_4 and applied to a specially prepared alumina column (vide infra). The column was eluted with oxygen-free methanol (1%) in benzene to afford the fractions containing **8e** alone. The fractions were combined and evaporated to dryness to give pure **8e**: λ_{max} (benzene) 420, 446, 539 nm. The electronic spectrum of **8e** indicates no contamination with oxy-, μ-oxo dimer or other impurities.

Preparation of the Alumina Column. A suspension of 4 g of neutral alumina (Wolem activity I) and 0.15 g of $Na_2S_2O_4$ in 20 mL of deoxygenated H_2O was stirred for 30 min under Ar atmosphere. Alumina was collected by decantation, washed with deoxygenated H_2O (6 × 10 mL), and dried in vacuo (1 × 10^{-3} torr, at room temperature) for 12 h. The pretreated alumina was placed into a column and used for the purifications of bisferrous gable porphyrin. To remove trace oxygen adsorbed on alumina, 1 mL (ca. 1 × 10^{-4} M) of benzene solution of bisferrous gable porphyrin was passed through the column by use of benzene–methanol (100:1) as an eluent just before use.

Measurement of Base Binding Equilibria. Because of the extreme oxygen sensitivity of ferrous porphyrins in solution, the 4-coordinate (baseless) ferrous porphyrins were freshly prepared in the drybox just before use. In a typical experiment, 2.0 mg of Fe^{III}_2·gable Cl_2 was dissolved in benzene (5 mL) and 0.5 mL of buffer (0.1 M phosphate, pH 6.86) was added. The mixture was deoxygenated by freeze–pump–thaw cycles (three times, 2 × 10^{-6} torr), and 20 mg of solid $Na_2S_2O_4$ was added under Ar. After vigorous shaking for 30 min, the brown solution turned to an orange-red. The benzene layer was removed by pasteur pipet in the drybox filled with oxygen-free argon and dried over anhydrous Na_2SO_4. Ferrous gable porphyrin was purified through a special column pretreated with a reducing reagent (vide supra). λ_{max} (benzene) 420, 445, 534 nm. Equilibrium constants were determined by visible spectrophotometric titration. To a benzene solution (2.0 mL) of the bisferrous gable porphyrin was added 0.05–0.4 mL of the benzene solution of the axial ligand, and the total volume of each mixture was then adjusted to 2.5 mL by the addition of deoxygenated benzene. Then, the spectra were recorded at 18 °C in the 350–750 nm range.

Equilibrium constants for the base binding reaction of Co^{II}_2·gable and Zn^{II}_2·gable were similarly measured by a spectrophotometric titration method. Aliquots of a solution containing an appropriate amount of an axial ligand were added to a 1-mL solution of Co^{II}_2·gable or Zn^{II}_2·gable and the total volume was adjusted to 5 mL under an Ar atmosphere. The spectra were recorded at 18 °C in the 750–350 nm region.

Registry No. 8a, 85318-78-1; **8b**, 96481-87-7; **8c**, 96481-88-8; **8d**, 96502-29-3; **8e**, 96481-89-9; ZnTPP, 14074-80-7; CoTPP, 14172-90-8; DIM, 84661-56-3; 1-MeIm, 616-47-7; DPM, 60776-05-8; Pic, 108-89-4.

Synthesis and Characterization of Phenolate-Bridged Copper Dimers with a Cu–Cu Separation of >3.5 Å. Models for the Active Site of Oxidized Hemocyanin Derivatives

Thomas N. Sorrell,*[1a] Charles J. O'Connor,[1b] Oren P. Anderson,[1c] and Joseph H. Reibenspies[1c]

Contribution from the Departments of Chemistry, The University of North Carolina at Chapel Hill, Chapel Hill, North Carolina 27514, the University of New Orleans, New Orleans, Louisiana 70148, and Colorado State University, Fort Collins, Colorado 80523. *Received June 11, 1984*

Abstract: Described are the synthesis and characterization of the new binucleating ligand 2,6-bis(bis[2-(1-pyrazolyl)-ethyl]amino]-*p*-cresol (Hbpeac) and two of its copper(II) derivatives. The ligand provides four donors, including a bridging phenoxide, to each metal ion. An "exogenous" ligand completes the coordination sphere of each copper. Both the μ-acetato (**1a**) and the μ-1,3-azido (**1b**) copper(II) complexes have been characterized by X-ray crystallography. In both structures, the coordination spheres of the copper(II) ions are distorted from a square-pyramidal geometry toward a trigonal-bipyramidal arrangement. The distortion is more pronounced in the acetato complex and accounts for the difference between the two compounds in terms of their magnetic behavior. Variable temperature magnetic susceptibility measurements demonstrate strong antiferromagnetic coupling ($2J = -1800$ cm^{-1}) for the azido derivative but negligable magnetic interaction between the copper ions in the acetato complex. The magnetic behavior, electronic spectrum, and structure of the azide derivative suggest that this complex is an excellent structural model for the oxidized azide derivative of hemocyanin. Crystal data for $C_{32}H_{42}Cl_2Cu_2N_{10}O_{12}$ (**1a**) are as follows: orthorhombic, a = 13.999 (5) Å, b = 23.046 (9) Å, c = 12.523 (5) Å, V = 4043 Å^3, Z = 4, space group = $P2_12_12_1$. Crystal data for $C_{31}H_{41}Cl_2Cu_2N_{13}O_{13}$ (**1b**) are as follows: orthorhombic, a = 12.977 (2) Å, b = 13.188 (3) Å, c = 22.033 (6) Å, V = 3771 Å^3, Z = 4, space group = $P2_12_12_1$.

Hemocyanin (Hc)[2] is a copper-containing protein which functions to transport dioxygen in the hemolymph of several species of arthropods and mollusks. Its binuclear active site has been extensively characterized spectroscopically,[3,4] and its reactions have been used to generate many interesting inorganic species which until recently have had (or in some cases still have) no counterparts among synthetic complexes.[5]

(1) (a) University of North Carolina. (b) University of New Orleans. (c) Colorado State University.

(2) Abbreviations used in this paper: Hc, hemocyanin; HcO_2, oxyhemocyanin; bpeac, the anion of 2,6-bis(bis[2-(1-pyrazoyl)ethyl]amino)-*p*-cresol; DMF, dimethylformamide; OAc, acetate; THF, tetrahydrofuran.

(3) (a) Solomon, E. I. In "Copper Proteins"; Spiro, T. G., Ed.; Wiley: New York, 1981; Chapter 1. (b) Solomon, E. I.; Penfield, K. W.; Wilcox, D. E. *Struct. Bonding (Berlin)* **1983**, *53*, 1–57.

(4) (a) Woolery, G. L.; Powers, L.; Winkler, M.; Solomon, E. I.; Spiro, T. G. *J. Am. Chem. Soc.* **1984**, *106*, 86–92. (b) Wilcox, D. E.; Long, J. R.; Solomon, E. I. *Ibid.* **1984**, *106*, 2186–2194.

0002-7863/85/1507-4199$01.50/0

A number of workers have attempted to model fully oxidized hemocyanin derivatives, the so-called "met" forms, by using a chelating ligand that bridges two copper(II) ions with a phenolate group, but those ligands fail to separate the copper atoms by more than 3.1 Å because the ligand backbone contains six-membered chelate rings (A).[6] By analogy with Reed's μ-alkoxy dimer,[5] we

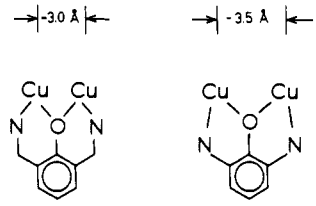

reasoned that five-membered chelates (B) would add more constraints, pulling the copper atoms to the desired separation of ca. 3.6 Å while increasing the Cu–O–Cu angle and promoting increased antiferromagnetic coupling. The latter point is noteworthy because both HcO_2 and met-azido Hc are very strongly antiferromagnetically coupled. We report here the synthesis and characterization of one such ligand and two of its copper derivatives. The μ-1,3-azido complex **1b** is the first reported diamagnetic μ-phenoxy copper dimer. Interestingly, there is no

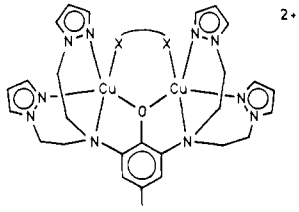

magnetic interaction between the copper centers in the acetato complex **1a**. Nevertheless, **1a** is important because its relatively simple electronic spectrum provides an explanation for the absence of resonance Raman-enhanced vibrational bands that would be expected if tyrosine is bound to copper in hemocyanin. Together, complexes **1a** and **1b** support the hypothesis that a tyrosinyl phenolate is the endogenous bridge at the hemocyanin active site.

Experimental Section

All reagents and solvents were purchased from commercial sources and used as received unless noted otherwise. Liquid ethylene oxide (Eastman Kodak) was purchased in sealed ampules that were opened after cooling, and the material was transferred as a liquid. Tetrahydrofuran (THF) was distilled from sodium benzophenone ketyl under nitrogen. 2,6-Diacetamido-4-methyl-1-phenyl acetate was prepared by the literature method.[7] Melting points were obtained with use of a Fisher-Johns apparatus and are uncorrected. Microanalyses were performed by MicAnal Laboratories, Inc., Tucson, AZ.

^{1}H NMR spectra were recorded on a Perkin-Elmer R-24B instrument at 60 MHz, a Varian XL-100 instrument at 100.1 MHz, or a Bruker WM 250 instrument at 250.13 MHz using $CDCl_3$ as the solvent. All chemical shifts are reported in parts per million (ppm) relative to an internal standard of Me_4Si. Electronic spectra were taken on a Hewlett-Packard 8450A rapid-scanning spectrophotometer.

2,6-Diacetamido-*p*-cresol. One-hundred grams of 2,6-diacetamido-4-methyl-1-phenyl acetate was stirred with a solution of 30 g of NaOH in 200 mL of water. After all the solid had dissolved, the solution was made acidic with concentrated hydrochloric acid. The precipitate was filtered, washed with water until the washings were colorless, and drried in air; mp 222–224 °C (lit.[7] 225 °C).

3,5-Diacetamido-4-(benzyloxy)toluene (2). Sodium metal (1.3 g, 56 mmol) was dissolved in 250 mL of absolute ethanol. Twelve grams of 2,6-diacetamido-*p*-cresol (54 mmol) was added to the solution followed by the addition of 7.2 g (57 mmol) of benzyl chloride and 1.7 g of sodium iodide. The solution was allowed to reflux for 5 h before it was poured onto ice. The mixture was made basic with NaOH, and the precipitate was filtered, washed with copious quantities of water, and air-dried. Crystallization from aqueous ethanol gave 11.6 g (69%) of white product: mp 182–185 °C (lit.[7] 185–186 °C); ^{1}H NMR δ 1.90 (6 H, s), 2.22 (3 H, s), 4.77 (2 H, s), 7.31 (7 H, m), 7.71 (2 H, s).

3,5-Bis[bis(2-hydroxyethyl)amino]-4-(benzyloxy)toluene (3). Potassium metal (8.4 g, 214 mmol) was dissolved in 350 mL of absolute ethanol under a dinitrogen atmosphere. Eleven grams of **2** (35 mmol) was then added, and the solution was allowed to reflux for 4 days. Ten milliliters of glacial acetic acid was then added, and the solution was evaporated at reduced pressure to give the air-sensitive diamino compound as an oil. The oil was dissolved in 450 mL of degassed (2:1) water–acetic acid, and the solution was cooled in an ice bath. Fifty milliliters of ethylene oxide was added in one portion and the solution allowed to stir at ambient temperature. After 24 h, the solution (which was now relatively stable to air) was concentrated at reduced pressure, treated with 10% NaOH, and extracted with several portions of methylene chloride. The extracts were washed with saturated sodium chloride solution and dried over Na_2SO_4. After removal of the drying agent and evaporation of the solvent, the crude product was purified by flash chromatography[8] by using ethyl acetate as the eluent. The ethyl acetate was evaporated, and the product was crystallized from ethyl acetate to give 6.0 g (42%) of white-to-pinkish crystals: mp 105.5–106.5 °C. Anal. C, H, N. ^{1}H NMR δ 2.26 (3 H, s), 3.26 (12 H, t, J = 5 Hz), 3.57 (8 H, t, J = 5 Hz), 4.95 (2 H, s), 6.73 (2 H, s), 7.27–7.49 (5 H, m).

3,5-Bis[bis[2-(1-pyrazolyl)ethyl]amino)-4-(benzyloxy)toluene (4). Compound **3** (1.9 g, 4.45 mmol) was added to a solution of 3.8 g (31.9 mmol) of thionyl chloride in 40 mL of methylene chloride. After 3 h, the solution was evaporated to an oil in a stream of N_2, 30 mL of CH_2Cl_2 was added, and the solution was again evaporated under nitrogen to give the crude chloride. In the meantime, 1.24 g (18.2 mmol) of pyrazole was dissolved under nitrogen in 75 mL of DMF in which 1.1 g of NaH had been suspended. After 1 h, the crude chloride from above was dissolved in 5 mL of DMF and added dropwise to the sodium pyrazolate solution. The mixture was allowed to stir for 4 days at 25 °C after which the excess NaH was destroyed by the careful addition of 10 mL of water. The solution was evaporated to dryness, the residue was dissolved in 10% NaOH, and the product was extracted with CH_2Cl_2. After the extracts were dried with Na_2SO_4, the crude mixture was purified by flash chromatography by using ethyl acetate as the eluent. The product, obtained as a viscous oil (R_f = 0.35 on silica gel), weighed 1.6 g (60%): ^{1}H NMR δ 2.26 (3 H, s), 3.60 (8 H, t, J = 6 Hz), 4.10 (8 H, t, J = 6 Hz), 4.37 (2 H, s), 6.13 (4 H, t, J = 2 Hz), 6.38 (2 H, s), 7.25 (4 H, d of d, J = 2, J' = 0.5 Hz), 7.30 (5 H, m), 7.45 (4 H, d of d, J = 2, J' = 0.5 Hz).

2,6-Bis(bis[2-(1-pyrazolyl)ethyl]amino)-*p*-cresol (Hbpeac) (5). The benzyl ether **4** (1.6 g, 2.7 mmol) was dissolved in a mixture of 15 mL of water and 10 mL of concentrated hydrobromic acid. The solution was allowed to reflux for 10 h, cooled to room temperature and neutralized to pH 7 with 10 M NaOH. The product was extracted with methylene chloride which was subsequently dried over Na_2SO_4. After filtration and evaporation of the solvent, the crude product was purified by flash chromatography by using ethyl acetate as the eluent (R_f = 0.2). The product, obtained as a viscous oil, weighed 0.9 g (65%): ^{1}H NMR δ 2.22 (3 H, S), 2.61 (1 H, s), 3.42 (8 H, t, J = 6 Hz), 4.07 (8 H, t, J = 6 Hz), 6.18 (4 H, t, J = 2 Hz), 6.64 (2 H, s), 7.25 (4 H, d, J = 2 Hz), 7.49 (4 H, d, J = 2 Hz).

μ-*O*,*O'*-Acetato[2,6-bis(bis[2-(1-pyrazolyl)ethyl]amino)-*p*-cresolato]-dicopper(II) Bis(perchlorate) (Acetonate), $[Cu_2(bpeac)(AcO)][ClO_4]_2 \cdot CH_3COCH_3$ (1a). A solution of 1.2 g (2.3 mmol) of Hbpeac in 20 mL of methanol was treated with a solution of 1.73 g (4.7 mmol) of $Cu(ClO_4)_2 \cdot 6H_2O$ in 20 mL of methanol. The resulting brown-purple solution was treated with 0.38 g (4.7 mmol) of sodium acetate which resulted in the formation of a bright-green solution. Addition of isopropyl alcohol gave 1.1 g of crude product after the solution stood overnight.

(5) The only derivative of hemocyanin that has been modeled successfully in terms of spectroscopic similarities is the met-azide form: McKee, V.; Zvagulis, M.; Dadgegian, J. V.; Patch, M. G.; Reed, C. A. *J. Am. Chem. Soc.* **1984**, *106*, 4765–4772.

(6) (a) Sorrell, T. N.; Jameson, D. L.; O'Connor, C. J. *Inorg. Chem.* **1984**, *23*, 190–195. (b) Karlin, K. D.; Hayes, J. C.; Gultneh, Y.; Cruse, R. W.; McKown, J. W.; Hutchinson, J. P.; Zubieta, J. *J. Am. Chem. Soc.* **1984**, *106*, 2121–2128. (c) Karlin, K. D.; Hayes, J. C.; Hutchinson, J. P.; Zubieta, J. *J. Chem. Soc., Chem. Commun.* **1983**, 376–378. (d) Robson, R. *Inorg. Nucl. Chem. Lett.* **1970**, *6*, 125. (e) Robson, R. *Aust. J. Chem.* **1970**, *23*, 2217. (f) Pilkington, N. H.; Robson, R. *Ibid.* **1970**, *23*, 2225–2236. (g) Hoskins, B. F.; Robson, R.; Schaap, H. *Inorg. Nucl. Chem. Lett.* **1972**, *8*, 21. (h) McFadyen, W. D.; Robson, R.; Schaap, H. *Iorg. Chem.* **1972**, *11*, 1777. (i) Hoskins, B. F.; Robson, R.; Vince, D. *J. Chem. Soc., Chem. Commun.* **1973**, 392. (j) Dickson, E.; Robson, R. *Inorg. Chem.* **1974**, *13*, 1301. (k) Hoskins, B. F.; Robson, R.; Williams, W. A. *Inorg. Chim. Acta* **1976**, *16*, 121. (l) McFayden, W. D.; Robson, R. *J. Coord. Chem.* **1976**, *5*, 49. (m) Gagnê, R. R.; Kreh, R. P.; Dodge, J. A. *J. Am. Chem. Soc.* **1979**, *101*, 6917–6927. (n) Grzybowski, J. J.; Merrel, P. H.; Urbach, F. L. *Inorg. Chem.* **1978**, *17*, 3078–3082. (o) Okawa, H.; Tokii, T.; Nonaka, Y.; Muto, Y.; Kida, S. *Bull. Chem. Soc. Jpn.* **1973**, *46*, 1462–1465.

(7) Saxena, M. P.; Ahmed, S. R. *Indian J. Technol.* **1971**, *9*, 37–38.

(8) Still, W. C.; Kahn, M.; Mitra, A. *J. Org. Chem.* **1978**, *43*, 2923–2925.

Table I. Crystallographic Details

complex	**1a**	**1b**
formula	$C_{32}H_{42}Cl_2Cu_2N_{10}O_{12}$	$C_{31}H_{41}Cl_2Cu_2N_{13}O_{10}$
temp, K	293	130
space group	$P2_12_12_1$	$P2_12_12_1$
a, Å	13.999 (5)	12.977 (2)
b, Å	23.046 (9)	13.188 (3)
c, Å	12.523 (5)	22.033 (6)
V, Å^3	4040	3771
Z	4	4
ρ, g/cm^3 (calcd)	1.57	1.68
cryst size, mm	0.20 × 0.20 × 0.50	0.40 (100 → $\bar{1}$00) × 0.12 (001 → 00$\bar{1}$) × 0.28 (010 → 0$\bar{1}$0)
collect range	$+h,+k,+l$ $2.0° \le 2\theta \le 50.0°$	$+h,-k,-l$ $3.5° \le 2\theta \le 50.0°$
transmission factors		
min	0.86	0.65
max	1.00	0.85
abs coeff, cm^{-1}	13.0	13.5
no. of data	3993	3706
no. of data [$I \ge 2\sigma(I)$]	2316	3093
R	0.093	0.071
R_w	0.069	0.067

The crude product was dissolved in acetone, treated with isopropyl alcohol, and allowed to stand for several days to give large green prisms of the product. Anal. $C_{32}H_{42}Cl_2Cu_2N_{10}O_{11}$: C, H, N.

μ-1,3-Azido[2,6-bis(bis[2-(1-pyrazolyl)ethyl]amino)-*p*-cresolato]dicopper(II) Bis(perchlorate) (Tetrahydrofuranate), [Cu$_2$(bpeac)(N$_3$)][ClO$_4$]$_2$·THF (1b). A solution of 0.15 g (0.3 mmol) of Hbpeac in 20 mL of methanol was treated with 0.22 g (0.6 mmol) of $Cu(ClO_4)_2 \cdot 6H_2O$. After solution was complete, 0.02 g (0.3 mmol) of sodium azide in 1 mL of water was added. The homogeneous emerald-green solution was treated with 50 mL of isopropyl alcohol and allowed to stand for 2 days. The crystalline product was collected, washed with isopropyl alcohol, and dried: yield 0.12 g (45%). Anal. Calcd for $C_{27}H_{33}Cl_2Cu_2N_{13}O_9$: C, 36.78; H, 3.77; N, 20.65; Cl, 8.04. Found: C, 36.82; H, 3.73; N, 19.78; Cl, 7.60. The crystals used for magnetic susceptibility studies and for the crystal structure were grown by vapor diffusion of THF into an acetonitrile solution of **1b** and contained a molecule of THF as a solvate.

X-ray Data Collection for 1a. A regularly shaped parallelepiped tube was sealed in a glass capillary, and a preliminary diffractometer search revealed orthorhombic symmetry. Systematic absences were observed which were consistent with the space group $P2_12_12_1$. Diffraction data were collected at 293 K on an Enraf-Nonius CAD-4 diffractometer using Mo Kα radiation (0.7107 Å) from a graphite crystal monochromator. The unit cell constants were derived from a least-squares refinement of the setting angles of 24 reflections. The $\omega - 2\theta$ scan technique was used to record the intensities. Peak counts were corrected for background counts, which were obtained by extending the final scan by 25% at each end to yield net intensities, I, which were assigned standard deviations calculated with a conventional ρ factor of 0.01. Intensities were corrected for Lorentz and polarization effects and showed no decay during the data collection. The data was further corrected for absorption effects by using an empirical correction based on psi scan data. Crystal data are given in Table I (crystallographic details).

Structure Determination and Refinement of 1a. A three-dimensional Patterson synthesis was used to locate the copper atom positions, and a series of difference Fourier maps revealed the remaining non-hydrogen atoms. The refinement was effected by full-matrix least-squares techniques. The function minimized was $\sum w(|F_o| - |F_c|)^2$ where $|F_o|$ and $|F_c|$ are the observed and calculated structure amplitudes, and the weight, w, is $4F_o^2/\sigma^2(F_o^2)$. Programs used for the structure solution and isotropic refinement were applied as a package by Enraf-Nonius. Atomic scattering factors for the non-hydrogen atoms were taken from ref 9 and those for hydrogen atoms from Stewart et al.[10]

Because of the size of the structure, the refinement was completed at the UNC Computation Center by using programs supplied by Hodgson.[11] All atoms in the cation except for the carbon atoms in the ethylene linkages, the benzene ring, and the acetato methyl group were refined anisotropically. Calculated, idealized hydrogen atom positions were included in the structure factor calculations. The hydrogen atoms on the aromatic, acetato, and acetone methyl groups were not included because of the uncertainty of their positions. When convergence of the atomic positions of the cation was reached, the atoms of the ClO_4^- groups were given anisotropic thermal parameters and were added to the refinement. Three of the oxygens of one of the perchlorate groups gave imaginary thermal parameters and could not be fit with any reasonable disordered model. The same was true for the solvate molecule; therefore, those atoms were refined isotropically. A final difference Fourier map revealed very little residual electron density (<0.2 e/Å^3). The final weighted R factor (on F) was 0.069 and the unweighted R factor was 0.093. Large thermal motion in one of the ClO_4^- groups and in the solvate molecule apparently results in the high R factor. Final positional parameters for **1a** are given in Table II, and distances and angles within the coordination

Table II. Final Positional Parameters for [Cu$_2$(bpeac)(OAc)][ClO$_4$]$_2$·Acetone (**1a**)

atom	x	y	z
Cu1	0.0845 (2)	0.4411 (1)	−0.0660 (2)
Cu2	0.1135 (2)	0.3361 (1)	−0.2721 (2)
Cl1	0.6609 (9)	0.4600 (5)	0.2331 (9)
Cl2	0.1517 (5)	0.2432 (3)	0.3660 (7)
OP1	0.7038 (26)	0.4525 (9)	0.3231 (21)
OP5	0.0657 (14)	0.2579 (9)	0.3971 (16)
OP6	0.1727 (10)	0.1866 (7)	0.4090 (14)
OP7	0.1648 (14)	0.2447 (8)	0.2547 (14)
OP8	0.2167 (13)	0.2844 (7)	0.4034 (20)
O1	0.0533 (9)	0.3740 (5)	−0.1476 (9)
OAC1	0.1857 (9)	0.4621 (5)	−0.1652 (12)
OAC2	0.2206 (10)	0.3893 (6)	−0.2654 (13)
CAC1	0.2378 (16)	0.4400 (10)	−0.2314 (16)
N1	−0.0280 (11)	0.4142 (7)	0.0261 (13)
N2	−0.0050 (10)	0.2792 (7)	−0.2586 (13)
N3	0.0678 (12)	0.5240 (7)	−0.0311 (11)
N4	0.0591 (16)	0.3807 (9)	−0.4012 (19)
N5	0.1896 (12)	0.4089 (7)	0.0515 (13)
N6	0.2097 (13)	0.2745 (9)	−0.3064 (12)
N3A	−0.0033 (11)	0.5503 (7)	0.0225 (12)
N4A	−0.0338 (17)	0.3841 (8)	−0.4264 (18)
N5A	0.1677 (13)	0.3829 (7)	0.1440 (15)
N6A	0.1899 (12)	0.2196 (8)	−0.3214 (15)
C3A	0.1316 (14)	0.5676 (9)	−0.0535 (16)
C3B	0.0955 (20)	0.6197 (8)	−0.0137 (17)
C3C	0.0110 (15)	0.6041 (9)	0.0338 (17)
C4A	0.0983 (22)	0.4169 (13)	−0.4774 (28)
C4B	0.0252 (34)	0.4424 (14)	−0.5433 (24)
C4C	−0.0528 (17)	0.4201 (15)	−0.5023 (27)
C5A	0.2848 (16)	0.4220 (9)	0.0537 (21)
C5B	0.3238 (15)	0.4044 (10)	0.1479 (23)
C5C	0.2460 (19)	0.3806 (8)	0.2068 (17)
C6A	0.3028 (15)	0.2794 (10)	−0.3090 (17)
C6B	0.3420 (15)	0.2268 (13)	−0.3308 (22)
C6C	0.2741 (24)	0.1886 (10)	−0.3346 (22)
C1A	−0.1042 (13)	0.4591 (8)	0.0163 (14)
C1B	−0.0800 (16)	0.5195 (9)	0.0654 (17)
C1C	0.0003 (13)	0.4094 (8)	0.1443 (16)
C1D	0.0716 (15)	0.3644 (8)	0.1640 (16)
C2A	−0.0679 (14)	0.2904 (9)	−0.3489 (16)
C2B	−0.1043 (15)	0.3508 (9)	−0.3649 (16)
C2C	0.0297 (12)	0.2168 (8)	−0.2523 (16)
C2D	0.0979 (17)	0.1997 (9)	−0.3361 (18)
CB1	−0.0182 (13)	0.3437 (8)	−0.1084 (15)
CB2	−0.0619 (12)	0.3609 (7)	−0.0153 (13)
CB3	−0.1405 (13)	0.3311 (8)	0.0255 (15)
CB4	−0.1697 (13)	0.2810 (8)	−0.0212 (14)
CB5	−0.1284 (13)	0.2636 (7)	−0.1137 (15)
CB6	−0.0512 (13)	0.2949 (8)	−0.1609 (15)
CBP	−0.2550 (14)	0.2442 (9)	0.0206 (16)
CAC2	0.3269 (12)	0.4697 (7)	−0.2668 (15)
OP2	0.6780 (20)	0.5075 (12)	0.1860 (23)
OP3	0.5742 (27)	0.4505 (18)	0.2229 (37)
OP4	0.6825 (23)	0.4113 (14)	0.1590 (26)
CS1	0.0722 (33)	0.1166 (19)	0.1201 (37)
OP4	0.6825 (23)	0.4113 (14)	0.1590 (26)
CS1	0.0722 (33)	0.1166 (19)	0.1201 (37)
CS2	0.0154 (24)	0.1548 (14)	0.0737 (30)
CS3	0.1740 (23)	0.0996 (13)	0.1344 (24)
OS1	0.0271 (18)	0.0805 (11)	0.1815 (21)

(9) "International Tables for X-ray Crystallography"; Kynoch Press: Birmingham, England, 1974; Vol. IV.

(10) Stewart, R. F.; Davidson, E. R.; Simpson, W. T. *J. Chem. Phys.* **1965**, *42*, 3175–3187.

(11) Singh, P.; Hodgson, D. J. *Acta Crystallogr., Sect. B* **1975**, *B31*, 845–851.

Table III. Bond Distances and Angles for the $Cu_2(bpeac)(OAc)^{2+}$ Cation

	Distances, Å		
Cu1–N1	2.046 (16)	Cu2–N2	2.120 (14)
Cu1–N3	1.974 (15)	Cu2–N4	2.062 (24)
Cu1–N5	2.209 (16)	Cu2–N6	2.004 (19)
Cu1–O1	1.905 (12)	Cu2–O1	1.976 (12)
Cu1–OAC1	1.946 (14)	Cu2–OAC2	1.940 (13)
Cu1–Cu2	3.562 (3)	O1–CB1	1.216 (19)
OAC1–CAC1	1.215 (19)	OAC2–CAC1	1.267 (23)
CAC1–CAC2	1.489 (26)		
	Angles, deg		
O1–Cu1–N1	83.1 (6)	O1–Cu2–N2	83.0 (6)
O1–Cu1–N3	151.4 (6)	O1–Cu2–N4	103.9 (6)
O1–Cu1–N5	103.7 (6)	O1–Cu2–N6	140.3 (6)
O1–Cu1–OAC1	91.5 (5)	O1–Cu2–OAC2	90.9 (6)
N1–Cu1–N3	94.5 (7)	N2–Cu2–N4	94.7 (7)
N1–Cu1–N5	92.0 (6)	N2–Cu2–N6	96.0 (7)
N1–Cu1–OAC1	174.2 (6)	N2–Cu2–OAC2	172.9 (7)
N3–Cu1–N5	104.9 (6)	N4–Cu2–N6	115.6 (7)
N3–Cu1–OAC1	89.3 (6)	N4–Cu2–OAC2	90.2 (8)
N5–Cu1–OAC1	91.4 (9)	N6–Cu2–OAC2	86.4 (7)
Cu1–O1–Cu2	133.2 (7)	Cu1–O1–CB1	113.9 (12)
Cu2–O1–CB1	112.6 (12)	Cu1–OAC1–CAC1	140.2 (15)
Cu2–OAC2–CAC1	138.2 (15)	OAC1–CAC1–CAC2	120.9 (22)
OAC2–CAC1–CAC2	118.9 (18)	OAC1–CAC1–OAC2	120.0 (24)

sphere are tabulated in Table III. Structure factors, thermal parameters, hydrogen atom positions, and ligand and anion distances and angles are included in the supplementary material (Tables S1-S5).

X-ray Data Collection for 1b. Many crystals were examined on the Nicolet *R3m* diffractometer at Colorado State University. Most were found to be unsatisfactory for data collection due to highly broadened peaks and satellite reflections. The dark-green crystal finally chosen for data collection was mounted on the end of a glass fiber and cooled in a stream of cold nitrogen to 130 K on the diffractometer. Diffraction data were collected on the Nicolet *R3m* diffractometer by using graphite-monochromated Mo Kα radiation (0.71073 Å). The cell constants reported in Table I were based on least-squares refinement of the setting angles of 25 reflections for which 2θ (av) = 13.7°. The orthorhombic symmetry suggested by the autoindexing routine was verified by axial photographs on the diffractometer.

The data were corrected for Lorentz and polarization effects, and the intensities for three check reflections showed no significant changes during the course of the data collection. The data were further corrected for absorption effects (analytical correction). Other details regarding data collection, data reduction, and structure solution and refinement are summarized in Table I (crystallographic details).

Structure Solution and Refinement for 1b. The positions of two independent copper atoms were obtained from the Patterson map. Atomic coordinates for all other non-hydrogen atoms were obtained from subsequent difference electron density maps. Near the end of this process, a molecule of tetrahydrofuran (THF) was discovered in the asymmetric unit. Programs used for the data reduction and structure determination and refinement were part of the SHELXTL program library, written by Prof. G. M. Sheldrick (University of Göttingen, FGR) and supplied by Nicolet XRD for the Data General Eclipse S/140 computing system at Colorado State University.

Least-squares refinement was carried to convergence, employing a model that included anisotropic thermal parameters for all non-hydrogen atoms except those of the cocrystallized THF molecule. Hydrogen atoms were included in idealized positions at fixed distances (0.96 Å) from the carbon atoms to which they are attached. At the conclusion of this portion of the refinement, R was 0.082 and R_w was 0.081. However, examination of a difference electron density map at this point revealed two prominent peaks ($\sim$3.0 e Å^{-3}) in the immediate vicinity of the two copper atoms of **1b**. In addition, examination of bond lengths and angles revealed significant differences in chemically equivalent parameters.

The origin of these two peaks is uncertain. It is possible that the cation is disordered to a minor extent, although the bulk of this species would seem to make such an explanation unlikely. It is possible that unresolved scattering from an undetected small twin fragment might cause such anomalous electron density to appear. Most likely, perhaps, is that these peaks reflect the cocrystallization of a minor amount of a structurally similar cationic impurity. This last possibility is favored by the fact that the magnetic susceptibility experiments revealed the presence of a small amount of a paramagnetic impurity (see below) in crystalline samples of this compound.

The prominence of these two peaks and the distance separating them ($\sim$3.7 Å, compared with the Cu1–Cu2 distance of $\sim$3.8 Å for the cation of **1b**) led to a decision to interpret them to be two copper atoms of a binuclear Cu(II)–bpeac cationic impurity. The structural model was then revised to accommodate these two copper atoms by allowing the site occupancy factor (SOF) for all atoms of the original cation to be refined (as a single number). The site occupancy factor for the pair of extra copper atoms was constrained to be 1.0 − SOF. At convergence, the value of SOF was 0.915. Because of the low level at which the extra cation was present (8.5%), other atoms of this disordered species were not discernible. The SOF's of the perchlorate counterions were fixed at 1.0 throughout the refinement.

SOF for the atoms of the THF molecule was refined to a value essentially equal to one and was fixed at 1.0 during the final stages of refinement. The large thermal parameters for the atoms of the THF molecule resulted in bond lengths which deviated significantly from expected values. As a consequence, the DFIX option of the SHELXTL refinement routine was used to fix the C–C and C–O bond lengths of this species to known values[12] while the atomic positions and thermal parameters were further refined.

The correctness of the enantiomorph assignment was checked by refinement of a multiplicative factor on the imaginary component of the anomalous scattering contribution. A strong indication was obtained that the reported enantiomorph was correct.

Inclusion of the minor contribution from the extra pair of copper atoms (with isotropic thermal parameters) in the final structural model improved the residual indexes (see Table I). More importantly, perhaps, most of the differences between chemically equivalent bond lengths that had been present earlier had disappeared by the time that the final convergence was reached. While some of the electron density is still missing (C, N, and O atoms of the impurity species), significant improvement over the previous structural model seems to have been achieved. The inability to assign this missing electron density undoubtedly accounts for the relatively high values of the final R factors. Final positional parameters for **1b** are given in Table IV, and distances and angles within the coordination sphere are tabulated in Table V. Structure factors, thermal parameters, hydrogen atom positions, and ligand and anion distances and angles are included in the supplementary material (Tables S6–S10).

Magnetic Measurements. Magnetic susceptibility data were recorded with a S.H.E. Corporation VTS superconducting SQUID susceptometer by using an IBM CS9000 minicomputer to drive the susceptometer instrument controller. The sample bucket was fabricated from an Al/Si allow obtained from S.H.E. Corp. The magnetic susceptibility of the sample bucket was measured independently over the entire temperature range, and the magnetic data for all samples was then corrected for the bucket contribution. Magnetic data were recorded over the indicated temperature range at a magnetic field setting of 5.00 kOe on polycrystalline samples weighing 100–130 mg. The magnetic susceptibility, corrected for diamagnetism by using Pascal's constants,[13] is listed in the supplementary material.

Results and Discussion

(A) Synthesis. Incorporation of five-membered chelates into the backbone of a ligand which would ultimately provide a phenolate bridge between two metal ions presented us with a task which had no literature precedent. The idea that nitrogen donors would need to be connected directly to the phenol ring suggested 2,6-dinitro-*p*-cresol as the logical starting material, and Scheme I illustrates the steps used to obtain the ligand Hbpeac. Hydrogenation, saponification, and benzylation were straightforward reactions giving the known amine **2** in a differentially protected form.[7] The amide groups were readily cleaved with ethoxide ion to give a very air-sensitive diamine which was converted without isolation to the tetrakis(hydroxyethyl) compound **3**. Conversion of the tetraalcohol to the tetrachloride with thionyl chloride immediately preceded a nucleophilic displacement reaction with pyrazolate ion to give the benzyl-protected ligand. The benzyl group was removed with aqueous HBr to yield the ligand after chromatography.

Stirring a solution of the ligand with copper(II) perchlorate gave a purple-brown solution containing, presumably, Cu_2-

(12) Huttner, G.; Gartzke, W.; Allinger, K. *J. Organomet. Chem.* **1975**, *109*, 47.

(13) O'Connor, C. J. *Prog. Inorg. Chem.* **1982**, *29*, 203–283.

Table IV. Final Positional Parameters for $[Cu_2(bpeac)(N_3)][ClO_4]_2 \cdot THF$ (**1b**)

atom	*x*	*y*	*z*
Cu1	0.7152 (1)	0.5760 (1)	0.8706 (1)
Cu2	0.9798 (1)	0.6213 (1)	0.9348 (1)
Cu1′	0.7334 (13)	0.6089 (13)	0.8431 (8)
Cu2′	0.9444 (6)	0.5707 (7)	0.9521 (4)
Cl1	0.3973 (2)	0.6489 (2)	0.7732 (1)
Cl2	0.2297 (2)	0.1632 (2)	0.9668 (1)
O1	0.8666 (4)	0.5555 (4)	0.8862 (3)
OP1	0.4582 (6)	0.6588 (7)	0.7206 (4)
OP2	0.4291 (7)	0.7241 (6)	0.8156 (4)
OP3	0.4135 (6)	0.5523 (5)	0.7992 (4)
OP4	0.2907 (5)	0.6602 (6)	0.7589 (4)
OP5	0.2616 (6)	0.0729 (7)	0.9953 (5)
OP6	0.1650 (6)	0.1469 (7)	0.9146 (4)
OP7	0.3146 (6)	0.2228 (6)	0.9496 (4)
OP8	0.1660 (8)	0.2132 (8)	1.0103 (4)
OT1	0.7872 (9)	1.0076 (2)	0.9122 (4)
N1	0.7304 (6)	0.4547 (6)	0.8139 (4)
N2	1.0729 (6)	0.5052 (6)	0.8998 (4)
N3	0.5804 (6)	0.5294 (6)	0.9054 (4)
N4	0.9969 (6)	0.5699 (5)	1.0255 (3)
N5	0.7050 (6)	0.6832 (6)	0.7976 (4)
N6	1.0778 (6)	0.7353 (6)	0.9180 (3)
N3A	0.5372 (6)	0.4387 (5)	0.8995 (4)
N4A	1.0027 (6)	0.4714 (6)	1.0372 (4)
N5A	0.7084 (6)	0.6575 (6)	0.7369 (3)
N6A	1.1828 (7)	0.7229 (6)	0.9063 (4)
NA1	0.7128 (6)	0.6922 (5)	0.9292 (4)
NA2	0.7919 (7)	0.7128 (6)	0.9488 (4)
NA3	0.8798 (7)	0.7270 (7)	0.9640 (5)
C1A	0.6791 (7)	0.3638 (6)	0.8447 (4)
C1B	0.5682 (8)	0.3728 (7)	0.8544 (5)
C1C	0.6840 (8)	0.4747 (7)	0.7552 (5)
C1D	0.7365 (8)	0.5530 (6)	0.7185 (4)
C2A	1.1000 (8)	0.4304 (8)	0.9457 (5)
C2B	1.0097 (8)	0.3981 (7)	0.9840 (5)
C2C	1.1707 (6)	0.5487 (7)	0.8715 (4)
C2D	1.2222 (9)	0.6271 (9)	0.9108 (5)
C3A	0.5257 (7)	0.5765 (9)	0.9473 (5)
C3B	0.4467 (8)	0.5144 (9)	0.9667 (6)
C3C	0.4566 (7)	0.4290 (9)	0.9357 (4)
C4A	0.9927 (7)	0.6190 (7)	1.0784 (4)
C4B	0.9992 (7)	0.5466 (8)	1.1245 (5)
C4C	1.0060 (8)	0.4553 (8)	1.0965 (5)
C5A	0.6835 (7)	0.7797 (8)	0.8000 (5)
C5B	0.6758 (8)	0.8194 (8)	0.7412 (6)
C5C	0.6923 (7)	0.7386 (8)	0.7047 (5)
C6A	1.0642 (10)	0.8327 (9)	0.9150 (5)
C6B	1.1536 (12)	0.8850 (11)	0.9022 (5)
C6C	1.2225 (11)	0.8108 (9)	0.8994 (6)
CB1	0.9040 (6)	0.4841 (6)	0.8503 (4)
CB2	0.8420 (6)	0.4339 (7)	0.8085 (4)
CB3	0.8787 (7)	0.3592 (6)	0.7711 (4)
CB4	0.9830 (7)	0.3354 (7)	0.7726 (4)
CB5	1.0453 (7)	0.3824 (8)	0.8141 (5)
CB6	1.0088 (7)	0.4568 (7)	0.8523 (4)
CBP	1.0238 (8)	0.2513 (9)	0.7306 (5)
CT1	0.7866 (6)	1.1132 (2)	0.9137 (7)
CT2	0.8930 (6)	1.1433 (7)	0.8876 (5)
CT3	0.9188 (14)	1.0604 (10)	0.8388 (7)
CT4	0.8435 (14)	0.9791 (13)	0.8610 (6)

$(bpeac)(S)_2^{3+}$, where *S* = methanol or water. Attempts to isolate this material have been unsuccessful. However, addition of sodium acetate or sodium azide led to the crystallization of the μ-*O,O′*-acetato or μ-1,3-azido derivatives as green, crystalline complexes.

(B) Molecular Structure of $[Cu_2(bpeac)(OAc)][ClO_4]_2$·acetone (1a). Compound **1a** crystallizes from acetone–isopropyl alcohol as bright-green prisims. Crystal data are given in Table I, final parameters are listed in Table II, and significant bond distances and angles in the coordination sphere are collected in Table III. The structure of the cation is shown in Figure 1, and the inner-coordination sphere is illustrated in Figure 2.

As expected, the copper–copper distance of 3.56 Å in **1a** is larger than that observed previously for related ligands having the amine

Table V. Bond Distances and Angles for the $Cu_2(bpeac)(N_3)^{2+}$ Cation

	Distances, Å		
Cu1–N1	2.036 (8)	Cu2–N2	2.097 (8)
Cu1–N3	2.007 (8)	Cu2–N4	2.119 (7)
Cu1–N5	2.142 (8)	Cu2–N6	2.004 (9)
Cu1–O1	2.017 (5)	Cu2–O1	2.013 (6)
Cu1–NA1	2.002 (8)	Cu2–NA3	2.011 (9)
Cu1–Cu2	3.765 (2)	Cu1′–Cu2′	3.678 (9)
O1–CB1	1.321 (10)	NA1–NA2	1.147 (12)
NA2–NA3	1.205 (13)		
	Angles, deg		
O1–Cu1–N1	84.5 (3)	O1–Cu2–N2	85.0 (3)
O1–Cu1–N3	138.2 (3)	O1–Cu2–N4	116.0 (3)
O1–Cu1–N5	106.1 (3)	O1–Cu2–N6	133.7 (3)
O1–Cu1–NA1	90.4 (3)	O1–Cu2–NA3	89.8 (3)
N1–Cu1–N3	94.5 (3)	N2–Cu2–N4	92.9 (3)
N1–Cu1–N5	93.8 (3)	N2–Cu2–N6	96.5 (3)
N1–Cu1–NA1	174.8 (3)	N2–Cu2–NA3	174.8 (4)
N3–Cu1–N5	115.7 (3)	N4–Cu2–N6	110.2 (3)
N3–Cu1–NA1	88.6 (3)	N4–Cu2–NA3	89.4 (4)
N5–Cu1–NA1	88.6 (3)	N6–Cu2–NA3	87.1 (4)
Cu1–O1–Cu2	138.2 (3)	Cu1–O1–CB1	110.6 (5)
Cu2–O1–CB1	110.8 (5)	Cu1–NA1–NA2	114.2 (7)
Cu2–NA3–NA2	114.6 (7)	NA1–NA2–NA3	172.1 (10)

Scheme I

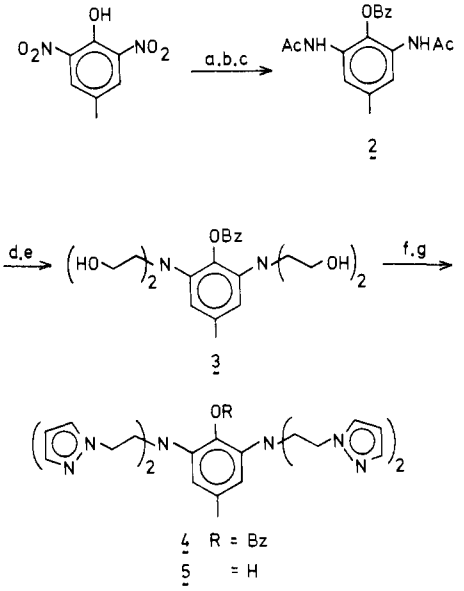

[a] H_2, PtO_2, Ac_2O, 25 °C, 4 days. [b] OH^-, 25 °C, 2 h/H^+. [c] NaOEt, EtOH/$C_6H_5CH_2Cl$, 25 °C, 6 h. [d] KOEt, EtOH, reflux, 4 days. [e] Ethylene oxide, 1:1 aqueous HOAc, 25 °C, 24 h. [f] $SOCl_2$, CH_2Cl_2, 25 °C, 2 h. [g] $NaC_3H_3N_2$, DMF, 25 °C, 4 days. [h] (4 → 5) HBr–H_2O (3:2), reflux, 10 h.

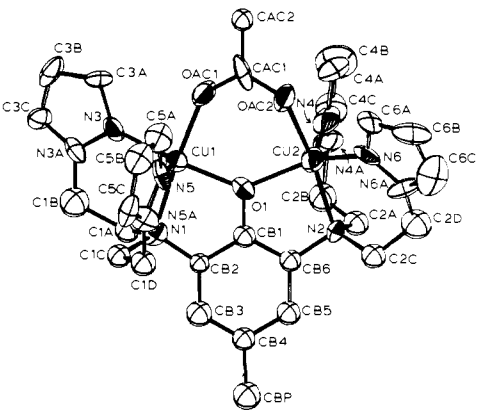

Figure 1. Structure of the $Cu_2(bpeac)(OAc)^{2+}$ cation showing 40% probability thermal elipsoids.

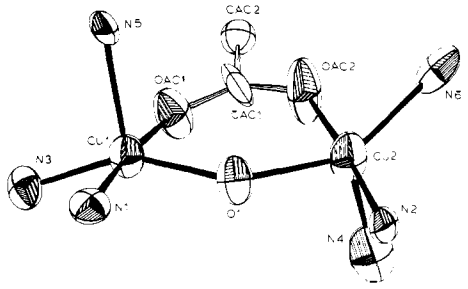

Figure 2. Coordination spheres of the copper ions in the $Cu_2(bpeac)(OAc)^{2+}$ cation. Distances and angles are given in Table III.

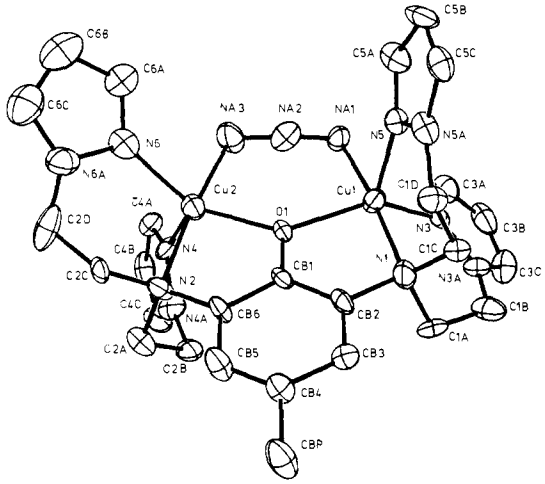

Figure 3. Structure of the $Cu_2(bpeac)(N_3)^{2+}$ cation showing 40% probability thermal elipsoids.

nitrogen separated from the phenol ring by an additional carbon.[6] Concomitant with the increase in the Cu–Cu distance is the opening of the Cu–phenolate–Cu angle from the ~103° observed for previous systems[6] to 133° for **1a**.

Because there is no symmetry imposed on **1a** crystallographically, each copper may assume a different geometry. Cu1 can be described as having a square-pyramidal geometry with the axial position defined by N5. Even this geometry is significantly distorted, and the four atoms defining the tetragonal plane deviate from that plane by an average of 0.2 Å. On the other hand, the geometry about Cu2 is less readily defined since Cu2–N4, which should correspond to the tetragonally elongated bond of a square pyramid, is actually shorter than Cu2–N2. Cu2 might be better described as a distorted trigonal-bipyramid, with the trigonal plane defined by O1, N4, and N6. It is interesting to note that the distortions observed for Cu2 are very similar to those seen for our previously reported μ-hydroxy copper dimer.[6a] In both complexes, the Cu–phenolate bond distances are also significantly different, with the longer Cu–O bond being formed with the copper distorted more toward the trigonal-bipyramidal geometry.

The ligand distances and angles show no unusual features, and only the disordered perchlorate ion and acetone solvate deviate from their expected geometries due to high thermal motion. Thus, although the final positions for those atoms account for the observed electron density, the resulting geometries are only approximate.

(C) Molecular Structure of $[Cu_2(bpeac)(N_3)][ClO_4]_2$·THF (1b). Compound **1b** crystallizes from acetonitrile–tetrahydrofuran as dark-green crystals. Crystal data are given in Table I, final parameters are listed in Table IV, and bond distances and angles in the coordination sphere are given in Table V. The structure of the cation is shown in Figure 3, and the inner-coordination sphere is shown in Figure 4.

The structure of **1b** differs from that for **1a** in that the two copper atoms in **1b** have very similar coordination geometries. Thus, the Cu1–O1 and Cu2–O1 bond distances in **1b** are equal, unlike those in **1a**, and each copper atom is bound to a pyrazole

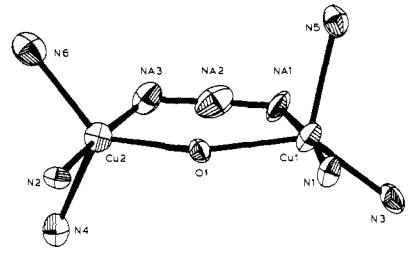

Figure 4. Coordination spheres of the copper ions in the $Cu_2(bpeac)(N_3)^{2+}$ cation. Distances and angles are given in Table V.

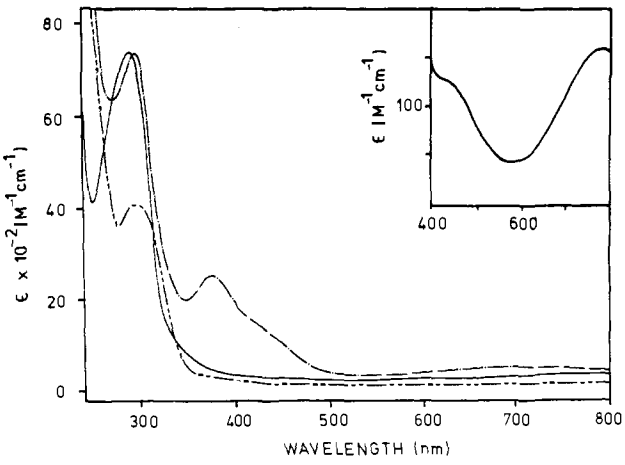

Figure 5. Electronic spectra of **1a** (—), **1b** (-·-·-), and the ligand Hbpeac (— — —) in methanol solution. The inset shows an expanded spectrum for **1a**.

nitrogen (N4 and N5) which is coordinated at a longer distance than the other donors in the coordination sphere. Therefore, we assign a tetragonal geometry to both copper atoms in **1b** which puts the phenolate bridge in a position to overlap with the $d_{x^2-y^2}$ orbital on each copper atom and leads to the observed diamagnetism (vide infra).

The copper–copper distance of 3.75 Å in **1b** is longer than that for **1a**, although this is probably due to the increased length of azide, a linear triatomic bridge, relative to acetate, a bent triatomic bridge. The distance is also about 0.1 Å longer than that found for metazidoHc by EXAFS spectroscopy[4] as well as for Reed's 1,3-azido-bridged copper dimer that has an alkoxide bridge.[5] A comparison of the bond lengths and angles within the coordination spheres of **1b** with those found by Reed for the μ-alkoxy complex shows their structures to be quite similar with like distortions away from a tetragonal geometry.

The Cu1–Na1 and Cu2–NA2 bond lengths in **1b** are the same within experimental error, averaging 2.006 (6) Å. The N–N bond lengths for the bridging azide ligand are in the range observed for other azido complexes[5,14] but appear to be significantly different from one another at 1.20 (1) and 1.15 (1) Å. The rather surprising nature of this result prompted a close examination of the van der Waals' contacts made by the cation of **1b**. This revealed that the packing about the cation is not symmetrical: for example, an oxygen atom of one of the perchlorate ions is the closet nonbonded atom to both copper atoms but is 3.6 Å from Cu1 and 4.1 Å from Cu2. It was not possible, however, to find a specific interaction that could cause the observed asymmetric in the azide bridge. The difference may not be as large as the final metric parameters suggest, given the problems encountered in the final stages of refinement of this structure (see Experimental Section). A spectroscopic check on this apparent inequivalency in bond length is possible since Solomon[4] has suggested that inequivalent N–N bond lengths in met-azido Hc account for the observation of two azide vibrational bands when isotopically labeled azide is used

(14) Agnus, Y.; Louis, R.; Gisselbrecht, J.-P.; Weiss, R. *J. Am. Chem. Soc.* **1984**, *106*, 93–102.

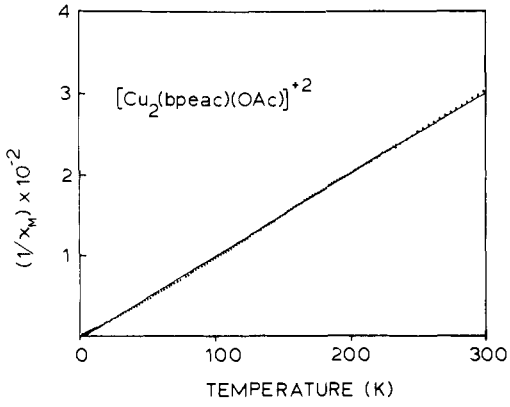

Figure 6. Plot of the inverse corrected molar magnetic susceptibility (in cgs units) for $Cu_2(bpeac)(OAc)(ClO_4)_2$·acetone as a function of temperature (in K). The points are the experimental data points, and the solid line is the result of the least-squares fitting of the parameters with the Curie-Weiss law to the data.

to prepare that derivative. A study of the mixed-isotope azide derivative of **1b** by Solomon's group is currently in progress.

(D) Spectroscopy. The visible spectra for complexes **1a** and **1b** are presented in Figure 5 along with that for the ligand Hbpeac. Both complexes exhibit a strong pyrazole → copper(II) charge-transfer transition near 300 nm (ϵ = 7400 M^{-1} cm^{-1} for **1a** and 7500 M^{-1} cm^{-1} for **1b**) and much weaker d–d transitions at lower energy (**1a**, λ_{max} = 778 nm, ϵ = 163 M^{-1} cm^{-1}; **1b**, λ_{max} = 682 nm, ϵ = 580 M^{-1} cm^{-1}). The spectrum of the free ligand shows a transition around 300 nm also, but that peak is weaker than those for the complexes. Schugar has demonstrated that Cu(II)–pyrazole complexes show strong charge-transfer transitions in this region;[15] therefore, we expect the 300-nm peak observed for the complexes to be predominantly due to CT transitions. The principal difference between the spectra is apparent for that of the azido complex which shows strong bands around 400 nm due to azide → copper(II) charge-transfer transitions. While there should be four N_3 → Cu(II) CT bands for a bridged binuclear complex,[3] these are not resolved. Instead one observes only a broad band at 376 nm (ϵ = 4600 M^{-1} cm^{-1}) with a low-energy shoulder (λ_{max} = 444 nm, $\epsilon \simeq$ 2000 M^{-1} cm^{-1}).

The argument has been presented that the band at ca. 425 nm observed for hemocyanin derivatives (especially for oxy Hc at 15 K)[3] is due to a phenolate → copper(II) CT transition.[3b] However, previously reported five-coordinate μ-phenolato–copper(II) dimers generally show a strong transition at higher energy (360–390 nm, $\epsilon \simeq 10^3$ M^{-1} cm^{-1}) associated with the phenolate CT transition.[6] Mononuclear Cu(II)–phenolate complexes, on the other hand, have phenolate → copper CT bands anywhere in the region of 350–500 nm with extinction coefficients of ca. 10^3 M^{-1} cm^{-1}.[3b] The μ-acetato complex **1a** presents an interesting case because it has no CT features associated with the "exogenous" acetate ion; therefore, the phenolate charge-transfer band should be observed. A band is observed at 446 nm with an extinction coefficient of only 122 M^{-1} cm^{-1} (see inset spectrum, Figure 5), and resonance Raman studies show enhancement of the phenolate C–O stretch at 1306 cm^{-1} when excitation is carried out at 457.9 nm.[16] Why this transition is so weak and has been shifted to lower energy compared to our previously reported copper dimer[6a] is at present uncertain; however, it may be due to the opening of the Cu–O–Cu angle which could lead to decreased overlap between the phenolate oxygen and copper orbitals.

In contrast to the acetate derivative, the azido complex **1b** shows no band that can be assigned unambiguously to the phenolate → copper CT transition. We presume that such a band is hidden by the more intense N_3^- → Cu CT transition around 444 nm; on that assumption we attempted to observe the C–O stretch in the resonance Raman spectrum of **1b**. Unfortunately, no spectrum could be obtained because of intense fluorescence from the sample.

The infrared spectrum for **1b** is notable only because of the strong asymmetric azide stretch which is seen at 2032 cm^{-1}. This value is in the range observed for other azidocopper(II) complexes; therefore it cannot be used to distinguish between the 1,1 and 1,3 bridging modes.[6c]

(E) Magnetic Susceptibility. Compound 1a. A plot of $(\chi_M^{corr})^{-1}$ vs. temperature for solid $Cu_2(bpeac)(OAc)(ClO_4)_2$·acetone is shown in Figure 6. The data are well fit by the Curie–Weiss law, and the solid line shows a least-squares fit to the expression $\chi_M^{corr} = C/(T-\theta)$ where $C = Ng^2\beta^2/4K$. The calculated g value is 2.25, typical for copper(II), and θ = 2.7°. The experimental susceptibility data are given in Table S11.

The negligible magnetic interaction between the two copper ions in **1a** suggests that at least one of the coppers must be distorted to the extent that its half-filled orbital cannot interact with the phenolate bridge for strong magnetic coupling. This assumes that acetate cannot promote coupling either, and that situation has precedent in the related μ-alkoxy-μ-acetato copper dimer reported by Reed.[5] In that system, the copper ions are trigonal bipyramidal, therefore have $(d_{z^2})^1$ ground states. The d_{z^2} orbitals are aligned with the acetato bridge yet there is little magnetic interaction.

In the present system, the crystal structure suggests that Cu1 is tetragonal but that Cu2 is trigonal bipyramidal.[17] Thus, the phenolate can interact with the unpaired electron in the $d_{x^2-y^2}$ orbital on Cu1, but it does not overlap with the orbital having the unpaired electron on Cu2 (namely d_{z^2}) which is oriented toward the acetate group as shown in Figure 7a. The acetate group is able to interact with the unpaired electron on each copper ion by direct orbital overlap, however. The observed magnetic behavior

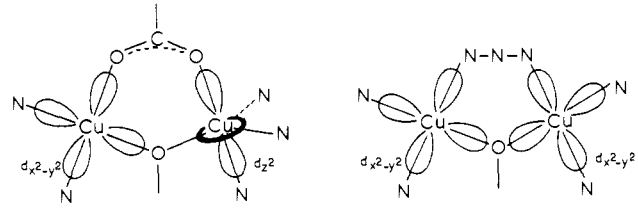

Figure 7. Schematic representation of the orbital orientations in complexes **1a** (a, left) and **1b** (b, right). The axial Cu–N bond of the tetragonal copper atoms has been omitted for clarity but is perpendicular to the $d_{x^2-y^2}$ orbital shown.

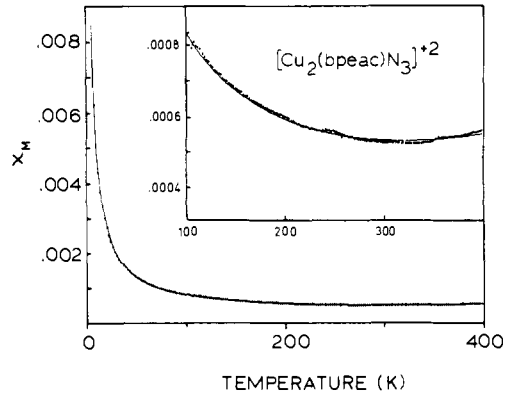

Figure 8. Plot of the corrected molar magnetic susceptibility (in cgs units) for $Cu_2(bpeac)(N_3)(ClO_4)_2$ as a function of temperature (in K). The solid line represents the result of the least-squares fitting of the parameters of eq 1 with the data.

(15) Bernarducci, E.; Schwindinger, W. F.; Hughey, J. L.; KroghJespersen, K.; Schugar, H. J. *J. Am. Chem. Soc.* **1981**, *103*, 1686–1691.

(16) We thank Prof. Larry Que for providing us with the resonance Raman results for **1a**. Complex **1b** was also examined but showed very strong fluorescence which obscured the vibrational modes. A full report on resonance Raman spectra of μ-phenolato copper dimers will be forthcoming from Prof. Que's group.

(17) EPR spectra of **1a** did not reveal the proposed d_{z^2} ground state for copper. In the solid state, a very broad band due to dipolar coupling was the only observed feature. In a frozen glass, a weak tetragonal signal was observed which we attribute to a small amount of monomeric impurity. We thank Prof. William Hatfield and Jeff Helms for obtaining these spectra.

for **1a** might be regarded as arising from an antiferromagnetic interaction mediated by the phenolate bridge through the torus of d_{z^2} on the trigonal-bipyramidal copper ion that is offset by a *ferromagnetic* interaction propagated via the acetato bridge, the latter phenomenon having been observed previously.[18]

Compound 1b. A plot of χ_M^{corr} vs. temperature for solid $Cu_2(bpeac)(N_3)(ClO_4)$ is presented in Figure 8, and the experimental data are listed in Table S12. The inset in Figure 8 reveals a 10-fold magnification of the high-temperature magnetic susceptibility data. Above 300 K, a very slight increase is observed in the magnetic susceptibility as the temperature is increased toward the 400 K susceptometer limit. The data listed in Table S12 and plotted in Figure 8 were recorded on a polycrystalline sample after it had experienced several 6–400 K temperature cycles. The reason for this is that the high-temperature magnetic data (300–400 K) for the first cycle were not reproducible and exhibited a great deal of scatter in that region. Most probably this resulted from evaporation of the THF from the crystal lattice since subsequent scans were reproducible over the entire temperature range, and no decomposition of the sample was detected at the elevated temperatures.

The extremely low value of the magnetic susceptibility observed for this complex would be expected for a spin-coupled binuclear molecule with a large antiferromagnetic coupling. The magnetic susceptibility of two interacting copper(II) ions may be described by eq 1 where $x = -2J/KT$ and $2J$ is the separation of the singlet

$$x = \frac{2Ng^2\mu\beta^2(e^x)}{KT(1 + 3e^x)} \quad (1)$$

and triplet energy levels; a negative J value denotes a ground-state singlet. The line drawn through the points in Figure 8 is obtained by using eq 1 and is corrected for a 3% paramagnetic impurity and a temperature-independent paramagnetism (TIP) of 0.00018 emu/mol for the two copper(II) ions. To obtain this curve, the values of g, TIP, and percent impurity were not varied, while J was allowed to change. The resulting values are $g = 2.10$, $2J = -1800$ cm^{-1}, TIP = 0.00018 emu/mol, and % paramagnetic impurity = 3.0.

Structurally, compound **1b** is similar to the μ-alkoxy-μ-azido copper dimer prepared by Reed.[5] That complex is reported to be diamagnetic at room temperature also, and the alkoxy bridge was deemed to be the primary superexchange pathway. The crystal structure for **1b** suggests that the phenolate is the likely pathway for coupling in this case since each copper is apparently tetragonal and overlap with the $d_{x^2-y^2}$ orbital on each would allow spin pairing as shown in Figure 7b. However, azide itself is able to promote strong antiferromagnetic coupling,[14] and a tetragonal ground state for the coppers in **1b** also places the azido bridge in a position to promote superexchange by overlap with the $d_{x^2-y^2}$ orbitals. It is interesting that the pentacoordinate copper complex made with our other binucleating ligand[6a] but having a 1,1-azide bridge in addition to the phenolate bridge shows a much weaker antiferromagnetic interaction, with $2J$ only about -450 cm^{-1}.[19]

(F) Conclusions and Summary. Solomon has proposed for hemocyanin that a tyrosinyl phenolate group bridges the two copper ions, promoting strong antiferromagnetic coupling between the metals in their oxidized state to produce a diamagnetic active site.[3] While there are examples of strongly coupled μ-phenolato copper(II) dimers,[3b,6] there are none that are diamagnetic at room temperature. Compound **1b** thus provides the first example of such a complex and confirms that phenoxide, like alkoxide[5] and hydroxide,[20] is a legitimate contender for the role of the endogenous bridge in coupled binuclear type III copper proteins. The fact that the spectroscopic and physical properties of **1b** match those for met-azidohemocyanin so closely strengthens the spectroscopically effective active site model of tetragonal copper(II) ions bridged by a phenolate group and a 1,3-azide ion.[3]

Additionally, the acetate complex reported here may explain why enhanced phenolate vibrational modes are not observed in the resonance Raman spectra of hemocyanin. The electronic spectrum for compound **1a** (vide supra) shows that the phenolate → copper charge-transfer band may be very weak in intensity, and enhancement of phenolate vibrations for the protein may be so slight as to be unobservable. For HcO_2, a peak seen at 425 nm which has been tenatively assigned as the phenolate → Cu CT band[3b] is also weak ($\epsilon \simeq 400$ M^{-1} cm^{-1}) and in fact is only well resolved at a temperature of 15 K.[3]

In summary, a new type of μ-phenolato copper(II) dimer has been prepared in which the copper ions are separated by more than 3.5 Å. Although very different from each other, the two complexes reported here illustrate two important points. First, the diamagnetism of the azide complex shows that the phenolate group is capable of mediating extremely strong antiferromagnetic coupling of the copper ions; second, the weakness of the phenolate → copper charge-transfer transition for the acetate derivative demonstrates for the first time that such bands may be difficult to observe in protein systems. Together, these results support the hypothesis that tyrosine is the endogenous bridge at the active site of hemocyanin.

Acknowledgment is made to the donors of the Petroleum Research Fund, administered by the American Chemical Society (TNS), to the Research Council of the University of North Carolina, to the National Science Foundation (TNS, CHE-8317080; CJO, CHE-8305707), and to the New Orleans Graduate Research Council for support of this research. The Nicolet *R3m* X-ray diffractometer and computational equipment at Colorado State University were purchased with funds from a grant of the National Science Foundation (CHE-8103011). Assistance with the crystallography of **1a** was generously provided by Prof. Derek Hodgson, and electronic spectra were obtained by A. S. Borovik.

Registry No. 1a, 96395-35-6; **1b**, 96411-94-8; **2**, 32498-75-2; **3**, 96395-31-2; **4**, 96395-32-3; **5**, 96411-91-5; 2,6-diacetamido-*p*-cresol, 32498-76-3; 2,6-diacetamido-4-methyl-1-phenyl acetate, 32498-77-4.

Supplementary Material Available: Tables S1–S5, including thermal parameters, hydrogen atom positions, ligand distances and angles, and values of F_{obsd} and F_{calcd} for **1a**, Tables S6–S10, including the same information for **1b**, and Tables S11 and S12, listing the susceptibility data for complexes **1a** and **1b**, respectively (47 pages). Ordering information is given on any current masthead page.

(18) Inoue, M.; Kubo, M. *Inorg. Chem.* **1970**, *9*, 2310–2316.
(19) Sorrell, T. N.; O'Connor, C. J.; Anderson, O. P.; Riebenspies, J. H., manuscript in preparation.
(20) Coughlin, P. K.; Lippard, S. J. *J. Am. Chem. Soc.* **1984**, *106*, 2328–2336.